DOI: 10.1002/chem.200700135

Copper Halide-Bridged Ruthenium Telluride Carbonyl Complexes: Discovery of the Semiconducting Cluster Chain Polymer $\{[PPh_4]_2[Te_2Ru_4(CO)_{10}Cu_4Br_2Cl_2]\cdot THF\}_\infty$

Minghuey Shieh,*[a] Miao-Hsing Hsu,[a] Wen-Shyan Sheu,[b] Li-Fing Jang,[a] Shu-Fen Lin,[a] Yen-Yi Chu,[a] Chia-Yeh Miu,[a] Yun-Wen Lai,[a] Hsiang-Lin Liu,[c] and Jim Long Her[c]

Abstract: A new series of Te–Ru–Cu carbonyl complexes was prepared by the reaction of K_2TeO_3 with $[Ru_3(CO)_{12}]$ in MeOH followed by treatment with PPh_4X (X = Br, Cl) and $[Cu(MeCN)_4]BF_4$ or CuX (X = Br, Cl) in MeCN. When the reaction mixture of K_2TeO_3 and $[Ru_3(CO)_{12}]$ was first treated with PPh_4X followed by the addition of $[Cu(MeCN)_4]BF_4$, doubly CuX-bridged Te_2Ru_4-based octahedral clusters $[PPh_4]_2[Te_2Ru_4(CO)_{10}Cu_2X_2]$ (X = Br, $[PPh_4]_2$[**1**]; X = Cl, $[PPh_4]_2$[**2**]) were obtained. When the reaction mixture of K_2TeO_3 and $[Ru_3(CO)_{12}]$ was treated with PPh_4X (X = Br, Cl) followed by the addition of CuX (X = Br, Cl), three different types of CuX-bridged Te–Ru carbonyl clusters were obtained. While the addition of PPh_4Br or PPh_4Cl followed by CuBr produced the doubly CuBr-bridged cluster **1**, the addition of PPh_4Cl followed by CuCl led to the formation of the Cu_4Cl_2-bridged bis-$TeRu_5$-based octahedral cluster compound $[PPh_4]_2[\{TeRu_5(CO)_{14}\}_2Cu_4Cl_2]$ ($[PPh_4]_2$[**3**]). On the other hand, when the reaction mixture of K_2TeO_3 and $[Ru_3(CO)_{12}]$ was treated with PPh_4Br followed by the addition of CuCl, the Cu(Br)CuCl-bridged Te_2Ru_4-based octahedral cluster chain polymer $\{[PPh_4]_2(Te_2Ru_4(CO)_{10}Cu_4Br_2Cl_2)\cdot THF\}_\infty$ ($\{[PPh_4]_2$[**4**]$\cdot THF\}_\infty$) was produced. The chain polymer $\{[PPh_4]_2$[**4**]$\cdot THF\}_\infty$ is the first ternary Te–Ru–Cu cluster and shows semiconducting behavior with a small energy gap of about 0.37 eV. It can be rationalized as resulting from aggregation of doubly CuX-bridged clusters **1** and **2** with two equivalents of CuCl or CuBr, respectively. The nature of clusters **1**–**4** and the formation and semiconducting properties of the polymer of **4** were further examined by molecular orbital calculations at the B3LYP level of density functional theory.

Keywords: carbonyl ligands · cluster compounds · copper · ruthenium · tellurium

Introduction

The rational synthesis, controllable structure, and special properties of supramolecular aggregates and extended networks constructed from soluble discrete units are currently a very active research area.[1–3] Recently, a number of extended solids have been constructed, primarily on the basis of coordination or organometallic complexes, and a promising new route to cluster-based frameworks by assembling metal cluster units from solution has emerged,[2f,3] because of their sizes, which start at the bottom end of the nanoregime, and their unique physical properties.[4,5] So far, such approaches, based on metal carbonyl clusters, have remained rare due to the intrinsic electron deficiency of most metal carbonyl clusters and the lack of available synthetic methodologies. Some notable examples, however, have been reported. For example, Scheer et al. used $[\{CpMo(CO)_2\}_2$-

[a] Prof. Dr. M. Shieh, M.-H. Hsu, L.-F. Jang, S.-F. Lin, Y.-Y. Chu, C.-Y. Miu, Y.-W. Lai
Department of Chemistry
National Taiwan Normal University
Taipei 116, Taiwan (Republic of China)
Fax: (+886) 2-2930-9081
E-mail: mshieh@ntnu.edu.tw

[b] Prof. Dr. W.-S. Sheu
Department of Chemistry
Fu-Jen Catholic University
Hsinchuang, Taipei 242, Taiwan (Republic of China)

[c] Prof. Dr. H.-L. Liu, J.-L. Her
Department of Physics
National Taiwan Normal University
Taipei 116, Taiwan (Republic of China)

Supporting information for this article is available on the WWW under http://www.chemeurj.org/ or from the author.

$(\mu,\eta^2\text{-}P_2)]$ and $[Cp^*Mo(CO)_2(\eta^3\text{-}As_3)]$ as efficient building blocks for the formation of polymers or aggregates with Ag^I and Cu^I salts.[3a,c,d] Wakatsuki et al. reported on a rare wire of clusters by treatment of the hexanuclear ruthenium carbonyl cluster anion with Ag^I ions.[3f] Recently, Longoni et al. isolated the 1D polymer $\{[Pt_9(CO)_{18}(\mu_3\text{-}CdCl_2)_2]^{2-}\}_\infty$ from the reaction of $[Pt_9(CO)_{18}]^{2-}$ with $CdCl_2$.[3g] Hence, the choice of appropriate metal carbonyl units, effective linkers, and feasible synthetic routes in this area is a great challenge.

Although some discrete Te–Ru carbonyl compounds were reported from solvothermal syntheses,[6] supramolecules or extended frameworks based on Te–Ru–CO remain scarce. The Te–Ru–CO compounds are of great importance due to their potential applications as catalysts and as precursors to some useful inorganic solid-state materials.[6,7] For example, the structure of $[Ru_6(Te_2)_7(CO)_{12}]^{2-}$ bears resemblance to its solid-state homologue Te_2Ru,[6a] which has been shown to exhibit a small optical energy gap of 0.491 eV compared to that of Si (1.170 eV).[7b] On the other hand, Cu^I, a soft Lewis acid, tends to form covalent bonds with soft bases, and this makes Cu^I ions potentially efficient linkers for connecting transition-metal carbonyl clusters to form polymeric or oligomeric frameworks.[3,8,9] Copper(I) ions also exhibit high conductivity when certain structural features are present in the compounds. With these perspectives and our continuing interest in carbonyl complexes containing heavier main-group elements and iron,[2g,10] manganese,[11] or chromium,[12] we recently initiated an exploratory study on the possibility of linking relatively soft Te–Ru carbonyl complexes with Cu^I salts with the goal of forming new ternary cluster complexes, which can further provide a broader spectrum of tunable properties and could be promising candidates for technical use.

Although the first example of Te–Fe–Cu complexes, $[TeFe_3(CO)_9(\mu\text{-}CuX)]^{2-}$,[13] was published, to the best of our knowledge, the synthesis of ternary Te–Ru–Cu clusters has not been reported. Here we report on the preparation of the first series of Te–Ru–Cu carbonyl clusters from reactions of K_2TeO_3 and $[Ru_3(CO)_{12}]$ followed by addition of PPh_4X and $[Cu(MeCN)_4](BF_4)$ or CuX (X = Br, Cl) in MeOH/MeCN. In addition, the rationalized aggregation, structural features, thermostability, and optical properties of the novel Te–Ru–Cu cluster chain polymer $\{[PPh_4]_2[Te_2Ru_4(CO)_{10}Cu_4Br_2Cl_2]\cdot THF\}_\infty$, are disclosed. The nature of this new series of Te–Ru–Cu clusters and the formation and semiconducting properties of the chain polymer were further investigated on the basis of DFT calculations.

Results and Discussion

Synthesis and structures of $[PPh_4]_2[Te_2Ru_4(CO)_{10}Cu_2X_2]$ (X = Br, $[PPh_4]_2$[1]; Cl, $[PPh_4]_2$[2]): While Te–Ru carbonyl clusters have been synthesized primarily by hydrothermal syntheses,[6] doubly CuX-bridged Te_2Ru_4-based octahedral clusters $[PPh_4]_2[Te_2Ru_4(CO)_{10}(\mu\text{-}CuX)_2]$ (X = Br, $[PPh_4]_2$[**1**]; X = Cl, $[PPh_4]_2$[**2**]) are readily obtained from the reaction of K_2TeO_3, $[Ru_3(CO)_{12}]$, PPh_4X, and $[Cu(MeCN)_4]BF_4$ in MeOH/MeCN (Scheme 1). Doubly CuBr-bridged cluster **1** could be isolated in high yield from the reaction of K_2TeO_3

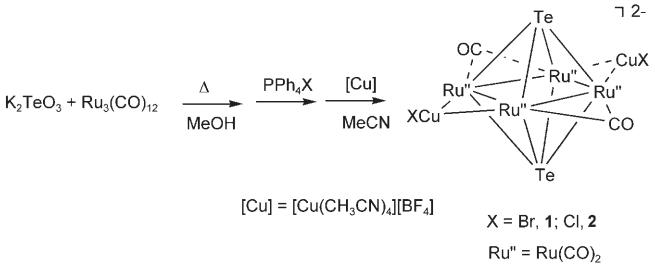

Scheme 1. Synthesis of **1** and **2** by reaction of K_2TeO_3 and $[Ru_3(CO)_{12}]$ with PPh_4X (X = Br, Cl) and $[Cu(MeCN)_4]BF_4$.

with $[Ru_3(CO)_{12}]$ in refluxing methanol followed by addition of PPh_4Br and $[Cu(MeCN)_4]BF_4$ in MeCN. The analogous CuCl-bridged cluster **2** was obtained in a similar fashion but with PPh_4Br being replaced by PPh_4Cl. Anionic clusters **1** and **2** can be isolated as the PPh_4^+ salts and were fully characterized on the basis of IR, elemental analysis, ESI-MS, and single-crystal X-ray analysis.

The X-ray analysis shows that the asymmetric units of $[PPh_4]_2$[**1**] and $[PPh_4]_2$[**2**] consist of two PPh_4^+ cations and one $[Te_2Ru_4(CO)_{10}Cu_2X_2]^{2-}$ dianion (X = Br, **1**; Cl, **2**). $[PPh_4]_2$[**1**] and $[PPh_4]_2$[**2**] are isomorphous, and the anionic complexes **1** and **2**, which have a crystallographic center of symmetry at the center of the Ru_4 plane, are shown in Figures 1 and 2, respectively. Complexes **1** and **2** each have a

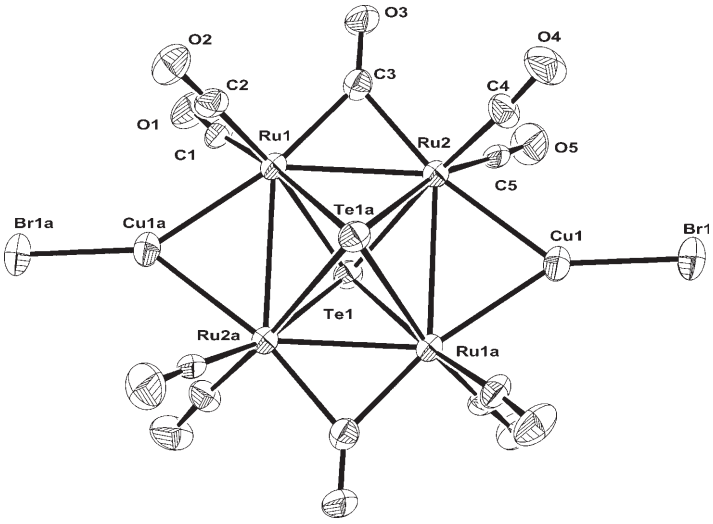

Figure 1. ORTEP diagram of anion **1**, showing 30% probability thermal ellipsoids.

octahedral Te_2Ru_4 cluster core with a rectangular Ru_4 plane, of which two opposite edges are bridged by carbonyl ligands and the other two edges are each bridged by a CuX unit (X = Br, **1**; Cl, **2**).

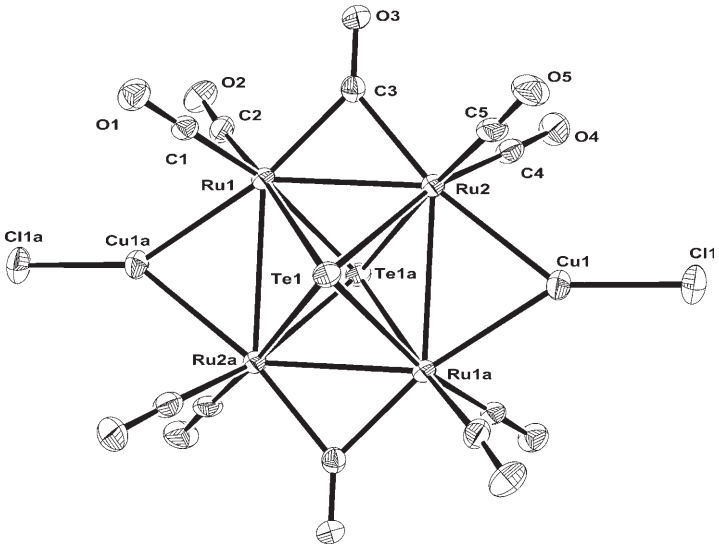

Figure 2. ORTEP diagram of anion **2**, showing 30% probability thermal ellipsoids.

Synthesis of $[PPh_4]_2$[3] and $\{[PPh_4]_2$[4]·THF$\}_\infty$: In the preparation of the Te_2Ru_4-based clusters **1** and **2**, the incorporation of halide from PPh_4X and Cu^I ions from $[Cu(MeCN)_4]BF_4$ into the Te–Ru clusters occurs and affects the outcome of the reaction. To further elucidate the role of PPh_4X and other Cu^I salts in analogous reactions, we carried out the reactions of K_2TeO_3 and $[Ru_3(CO)_{12}]$ with PPh_4X and CuX (X = Br, Cl) in various combinations (Scheme 2).

In the case of CuBr, when the reaction mixture of K_2TeO_3 and $[Ru_3(CO)_{12}]$ was treated with PPh_4Br or PPh_4Cl in MeOH followed by the addition of CuBr in MeCN, doubly CuBr-bridged cluster **1** was produced, as confirmed by IR spectroscopy and ESI-MS, and no chloride-incorporating product was isolated in the PPh_4Cl case. To better understand the effect of the order of addition of PPh_4X (X = Br, Cl) and CuBr, the reactions were carried out with reversed addition of PPh_4X and CuBr (i.e., first CuBr then PPh_4X). Interestingly, only the doubly CuBr-bridged cluster **1** was produced in both reactions, as confirmed by IR spectroscopy and ESI-MS, regardless of the order of the addition, and this indicates the strong affinity of CuBr for bridging the Ru–Ru edges in the Te_2Ru_4-based cluster core.

In the case of CuCl, when the reaction mixture of K_2TeO_3 and $[Ru_3(CO)_{12}]$ was treated with PPh_4Cl in MeOH followed by addition of CuCl in MeCN, the new Cu_4Cl_2-bridged bis-$TeRu_5$-based octahedral cluster compound $[PPh_4]_2$-$[\{TeRu_5(CO)_{14}\}_2Cu_4Cl_2]$ ($[PPh_4]_2$[**3**]) was produced (Figure 3). Surprisingly, the reaction of K_2TeO_3 and $[Ru_3(CO)_{12}]$ in MeOH followed by addition of PPh_4Br and CuCl in MeCN led to the formation of cluster polymer $\{[PPh_4]_2[Te_2Ru_4(CO)_{10}Cu_4Br_2Cl_2]\cdot THF\}_\infty$ ($\{[PPh_4]_2$[**4**]·$THF\}_\infty$). The anionic chain polymer made up of unit of **4** (Figure 4) can be viewed as being composed of Te_2Ru_4-based units that are further connected by two –Cu(Br)-CuCl– linkers. Clusters $[PPh_4]_2$[**3**] and $\{[PPh_4]_2$[**4**]·$THF\}_\infty$ were fully characterized by IR spectroscopy, elemental analysis, and single-crystal X-ray analysis. Reaction of K_2TeO_3 and $[Ru_3(CO)_{12}]$ with the addition of CuCl followed by either PPh_4Br or PPh_4Cl only resulted in the formation of the Cu_4Cl_2-bridged double-octahedral cluster **3**, which was confirmed by IR spectroscopy, elemental analysis, and single-crystal X-ray analysis. The tendency for the reactions of K_2TeO_3 and $[Ru_3(CO)_{12}]$ with PPh_4X and CuX (X = Br, Cl) with such subtle differences to produce clusters **1** and **3** and the polymer of **4** is surprising and intriguing. To summarize the results of the CuX/PPh_4X reactions (Scheme 2), it appears that CuBr can act as an effective edge-bridging ligand for the formation of Te_2Ru_4-based cluster **1** regardless of the order of its addition, whereas CuCl functions as a weaker edge-bridging ligand but has a coupling effect with PPh_4X to form either the Cu_4Cl_2-bridged bis-$TeRu_5$-based octahedral cluster **3** or the chain polymer of **4**, depending on the overall influences of PPh_4X and CuCl. However, the formation of **3** or **4** may rely on the addition of PPh_4X (X = Cl, Br) first, followed by CuCl in MeCN, and this suggests a critical role of PPh_4X salts in the case of CuCl.

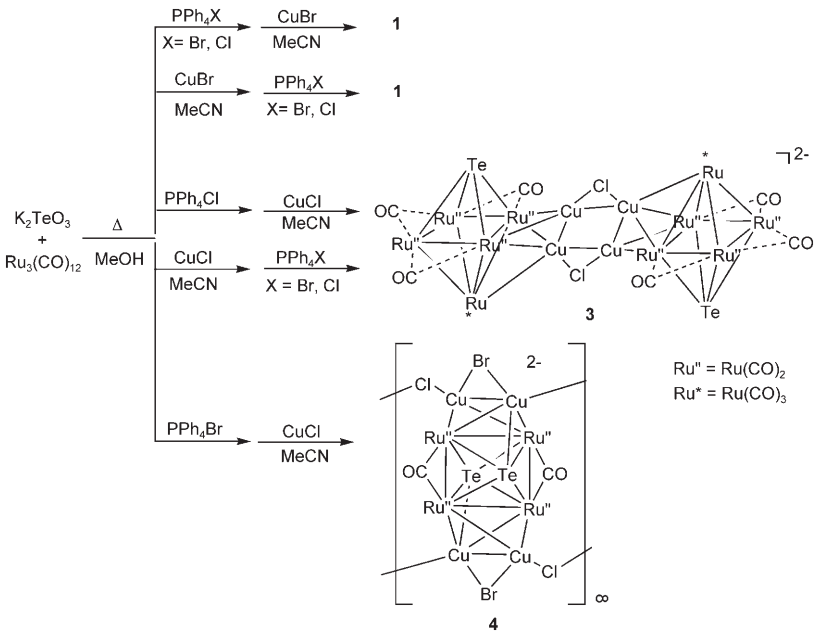

Scheme 2. Reactions of K_2TeO_3 with $[Ru_3(CO)_{12}]$ and PPh_4X/CuX (X = Br, Cl).

Structures of $[PPh_4]_2$[3] and $\{[PPh_4]_2$[4]·THF$\}_\infty$: The crystal structure of $[PPh_4]_2$[**3**] consists

of discrete cationic and dianionic units. There is no significant interaction between the cations and anions in $[PPh_4]_2$[**3**]. Dianion **3**, which has a crystallographic center of symmetry at the center of the Cu_4 parallelogram, is shown in Figure 3. Dianion **3** has two octahedral $TeRu_5$ units linked by a planar Cu_4 array, in which two opposite edges are bridged by chlorine atoms. Halide-bridged planar Cu_4 units are not common in the chemistry of Cu^I.[9] Cluster **3** is the first example of a halide-bridged Cu_4 unit as a linker connecting two Te–Ru clusters. In **3**, the Ru_4 planes of the two octahedra are almost perpendicular (87.88°) to the Cu_4 parallelogram, in which the two chloride-bridged Cu–Cu edges (2.779(1) Å) are longer than the other two edges (2.608(1) Å) due to the effect of the bridging chloride ions. In terms of charge distribution in **3**, the two $[TeRu_5(CO)_{14}]^{2-}$ units would provide four negative charges and two chloride ions two further negative charges, and each copper atom is assigned a formal charge of +1, which makes the complex a dianionic species, overall.

The X-ray analysis shows that the asymmetric unit of $\{[PPh_4]_2$[**4**]·THF$\}_\infty$ consists of two PPh_4^+ ions, one $[Te_2Ru_4(CO)_{10}Cu_4Br_2Cl_2]^{2-}$ ion, and one THF molecule. The anionic unit, which has a crystallographic center of symmetry at the center of the Ru_4 plane, is shown in Figure 4. The anionic unit (**4**) has an octahedral Te_2Ru_4 cluster core in which two opposite edges of the rectangular Ru_4 plane are bridged by carbonyl ligands and the other two edges are each linked by a Cu_2 unit that is further bridged by one Br atom and externally bonded to one Cl atom. As shown in Figure 5a, the anionic units are held together by chloride ions to form infinite metal cluster chains along the *b* axis. The chlorine atoms of the anions and the phenyl hydrogen atoms of the PPh_4^+ ions are involved in weak hydrogen bonding, which probably aids in the crystal packing of $\{[PPh_4]_2$[**4**]·THF$\}_\infty$ (Figure 5b). Along the *b* axis, zigzag arrays of anionic and cationic units wind around a 2_1 axis, whereby each cation acts as a linker to connect two anions together with H···Cl distances of 2.5880(1) and 2.8256(1) Å. The anionic units occupy eclipsed positions along the metal cluster chains, which exhibit two orientations with respect to the Ru_4 plane. While the chains along the *a* direction are parallel to each other, the adjacent ones along the *c* direction are in a staggered arrangement with a dihedral angle between two Ru_4 planes of 43°. Tetragonal-like channels between the cluster chains along the *b* direction are filled with THF molecules, each of which is surrounded by anionic and cationic units. The dimensions of these channels in the unit cell each vary from 5 to 6 Å with a half-THF volume of ap-

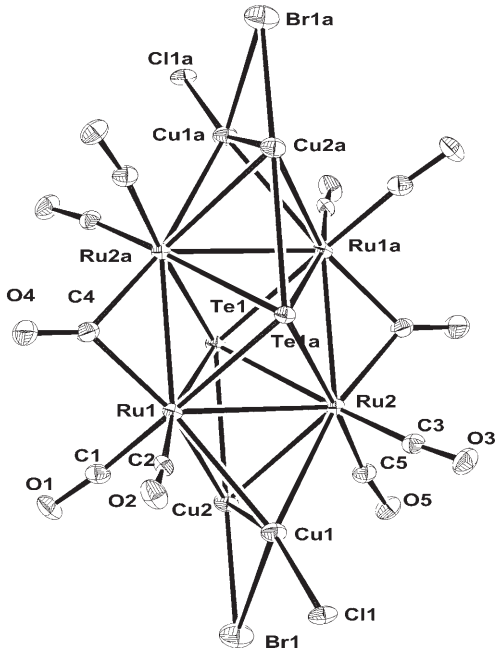

Figure 4. ORTEP diagram of the anionic unit of polymer $\{[PPh_4]_2$[**4**]·THF$\}_\infty$, showing 30% probability thermal ellipsoids.

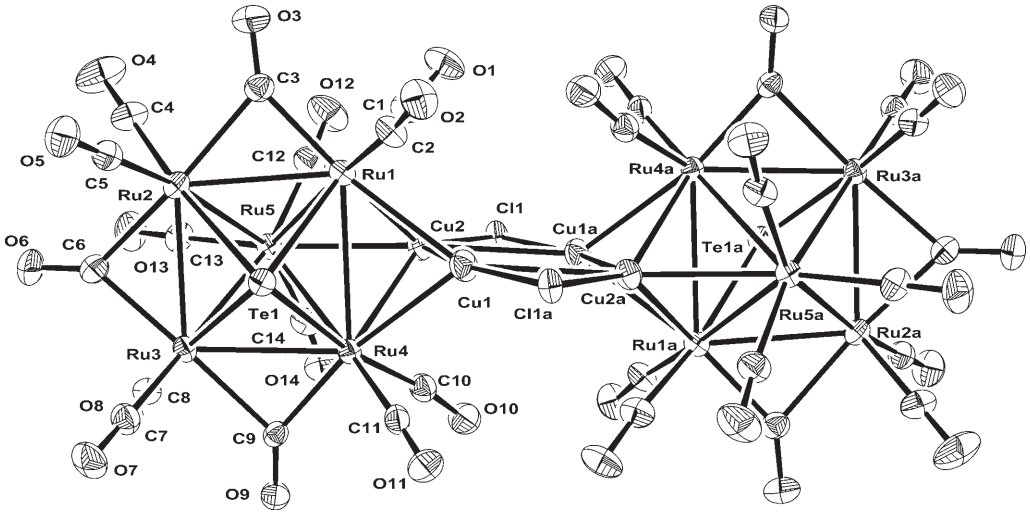

Figure 3. ORTEP diagram of anion **3**, showing 30% probability thermal ellipsoids.

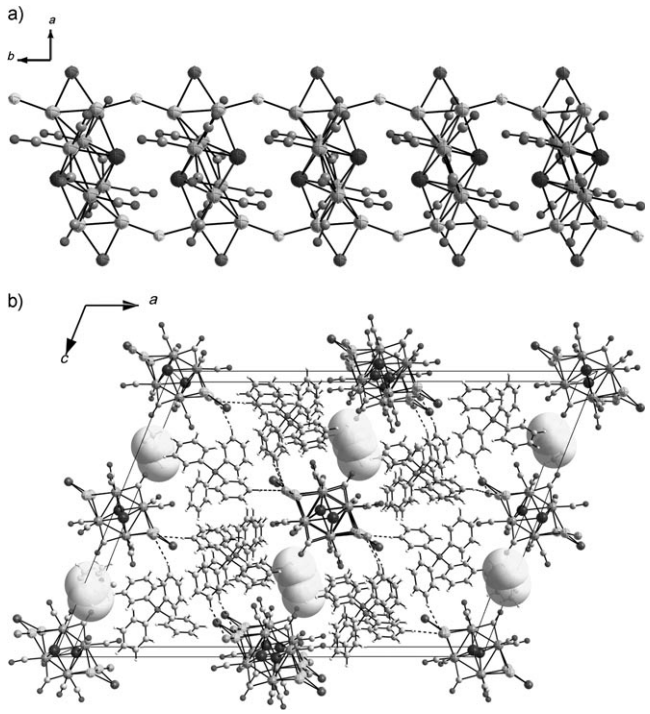

Figure 5. a) Section of the anionic polymer chain of $\{[PPh_4]_2[\mathbf{4}]\cdot THF\}_\infty$ and b) packing diagram of $\{[PPh_4]_2[\mathbf{4}]\cdot THF\}_\infty$ viewed down the *b* axis; the THF-filled cavities are represented by space-filling spheres.

proximately 118 Å^3 (based on calculations performed with PLATON[14]).

The thermal stability of polymer of **4** was evaluated by thermogravimetric analysis (TGA; see Supporting Information). The TGA of $\{[PPh_4]_2[\mathbf{4}]\cdot THF\}_\infty$ showed a gradual weight loss of 3.89% below 186°C, corresponding to the loss of THF molecules (theoretical 3.3%), and then a continuous weight loss of 44.86% up to 650°C, consistent with the loss of PPh_4^+ ions and CO ligands (theoretical 44%), to leave a residue with composition $Te_2Ru_4Cu_4Br_2Cl_2$. The result is indicative of the ease of loss of encapsulated THF molecules in **4** below about 200°C and the relative stability of the $Te_2Ru_4Cu_4Br_2Cl_2$ main framework.

Aggregation of $\{[PPh_4]_2[4]\cdot THF\}_\infty$: X-ray analysis showed that the anionic polymer of **4** is composed of a $Te_2Ru_4(CO)_{10}$ unit with two opposite Ru–Ru edges bridged by Cu(Br)CuCl moieties in a μ_2-η^2:η^2 manner (Figure 4). The polymer of **4** and clusters **1** and **2** are basically built from the $Te_2Ru_4(CO)_{10}$ unit. In a closer inspection of the structural relationship between **4** and the copper halide-bridged clusters **1** and **2**, the possibility arose that polymer of **4** could be synthesized rationally by treating complex **1** with CuCl or complex **2** with CuBr. To address this issue, we carried out reactions of complex **1** and **2** with CuCl or CuBr, respectively (Scheme 3). Indeed, when complex **1** or **2** was treated with two equivalents of linking agent CuX (X = Cl, Br, respectively) in MeCN under appropriate conditions, polymer **4** was isolated in reasonable yields with some

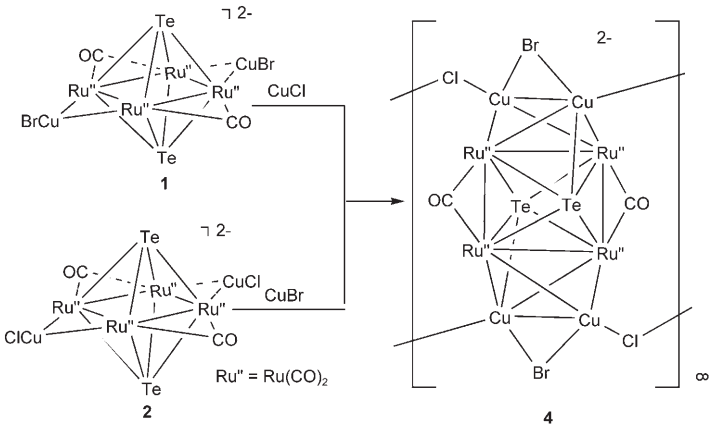

Scheme 3. Preparation of polymer **4** from **1** and CuCl or **2** and CuBr.

decomposition products. These results clearly demonstrate that polymer **4** can be rationally obtained by aggregation of complexes **1** and **2** with the appropriate CuX (X = Cl, Br). The formation of polymer **4** from both reactions is supported by IR spectroscopy, and the powder XRD patterns were identical to that derived from single-crystal X-ray diffraction (see Supporting Information). We believe that the fact that no analogous bromide-linked polymer is produced under our reaction conditions is due to the weaker ability of Br versus Cl to link two octahedron-based cluster units and the weaker H···Br versus H···Cl contacts, which are significant interactions for the crystal packing of $\{[PPh_4]_2[\mathbf{4}]\cdot THF\}_\infty$. However, given the lack of single-crystal X-ray data for the analogous bromide-linked polymer, its formation from this synthetic approach cannot be completely excluded.

Optical properties of $\{[PPh_4]_2[4]\cdot THF\}_\infty$: Near-normal optical reflectance spectra of single-crystal samples of polymer $\{[PPh_4]_2[\mathbf{4}]\cdot THF\}_\infty$ were obtained, and its optical properties [i.e., the complex conductivity $\sigma(\omega) = \sigma_1(\omega) + i\sigma_2(\omega)$] were calculated by Kramers–Kronig analysis.[15,16] To perform these transformations, it is necessary to extrapolate the reflectance at both low and high frequencies. At very low frequencies the reflectance was assumed to be constant. The high-frequency extrapolations were made with a weak power-law dependence $R \sim \omega^{-s}$ with $s \sim 1$–2.

Figure 6a shows the measured room-temperature optical reflectance over the entire frequency range (no polarization dependence was detected in the data). The spectrum displays a series of narrow structures associated with molecular vibrations at low frequencies and a broad maximum peak from electronic transitions at higher frequencies. The real part of the conductivity $\sigma_1(\omega)$, obtained from Kramers–Kronig analysis of the reflectance, is shown in Figure 6b. Overall, the sample exhibits semiconducting character, with a small residual conductivity (but no Drude-like response) in the far-infrared region. By extrapolating the frequency-dependent conductivity to zero frequency, the dc conductivity was estimated to be on the order of $(1\text{–}5) \times 10^{-2}\ \Omega^{-1}\,cm^{-1}$. The conductivity clearly increases at frequencies above

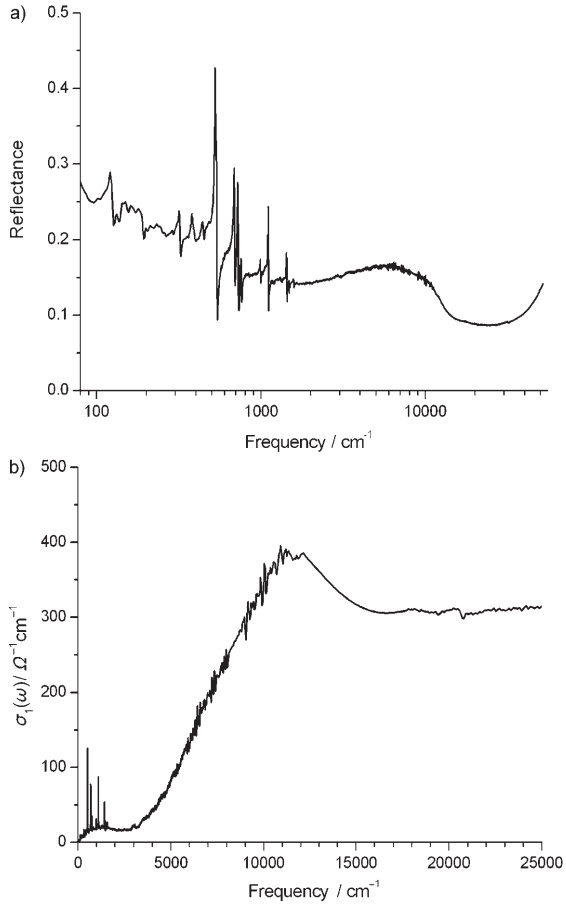

Figure 6. a) Room-temperature optical reflectance spectrum and b) room-temperature frequency-dependent optical conductivity of $\{[PPh_4]_2[\mathbf{4}]\cdot THF\}_\infty$.

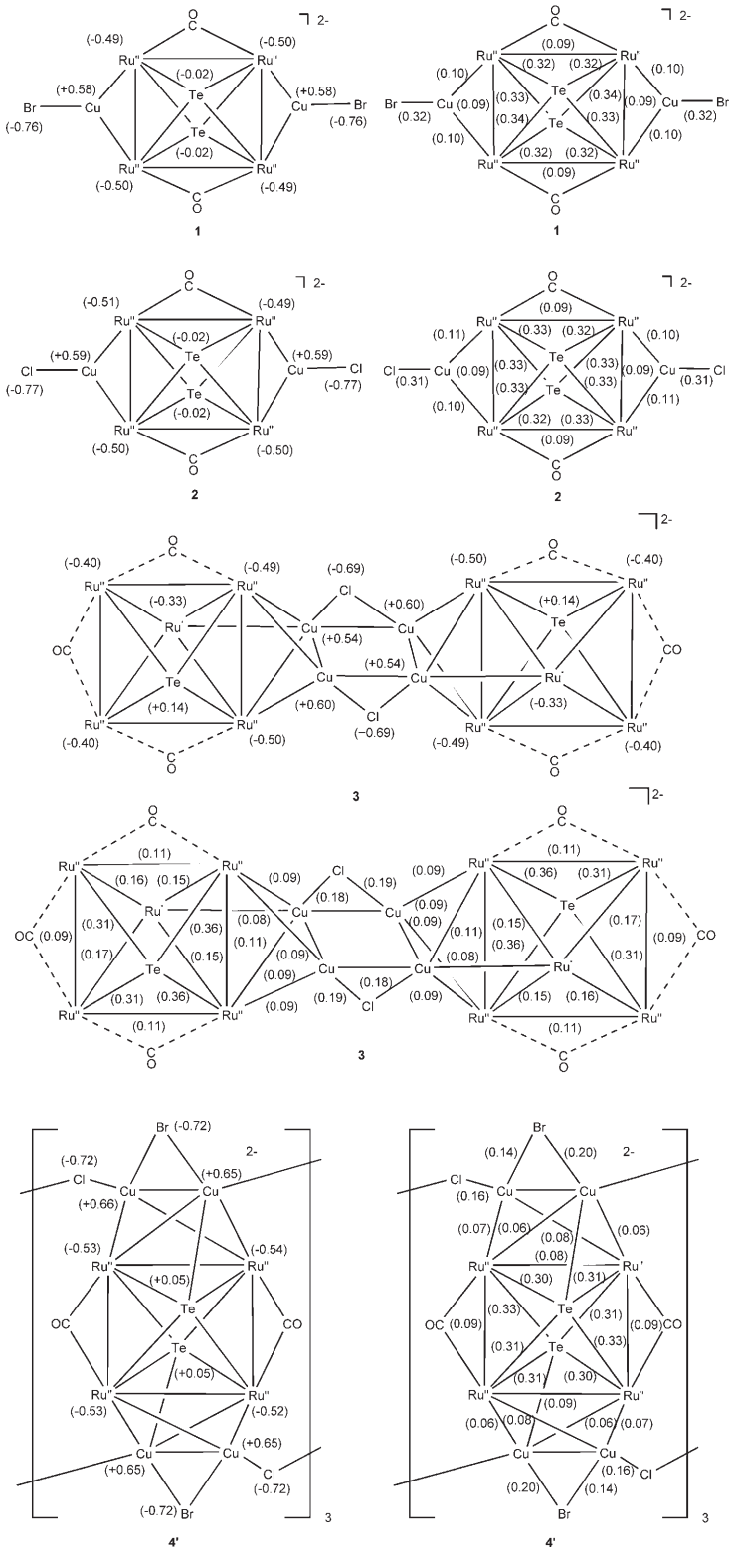

$3000\ cm^{-1}$ and reaches a peak around $11\,000\ cm^{-1}$. The onset frequency roughly corresponds to the energy gap ($E_g \approx 0.37$ eV $\approx 3000\ cm^{-1}$), which is smaller than that (0.491 eV) reported for Te_2Ru[7b] and suggests potentially enhanced conductivity of the Cu-containing Te–Ru phase.

DFT calculations: The DFT method was employed to understand the nature of clusters **1**–**4** and to rationalize the formation of polymer **4**. Molecular orbital calculations on complexes **1**–**4** were carried out at the B3LYP/LanL2DZ level of theory. As the original system of **4** is an infinite polymer chain, molecular fragments containing one to six $[Te_2Ru_4(CO)_{10}Cu_4Br_2Cl_2]^{2-}$ units were calculated to understand how polymer length affects the properties of the polymer. In addition, natural bond order (NBO) and natural population analyses (NPA) for complexes **1**–**3** and three units of polymer **4** were calculated and the results compared (Table 1).

The calculation shows that the active sites of **1** and **2** for the formation of **4** can be related to the electron density of the HOMO of complexes **1** and **2**. The Ru and halide atoms of **1** and **2** have significant negative charges (Table 1), which attract the positively charged Cu end of the incoming CuX towards the Ru_2CuX segments of complex **1** and **2**. The small Wiberg bond index of Ru–Cu (0.10) indicates that the bond is weak and that the CuX fragments of **1** and **2** are subject to rearrangement when they experience repulsive Cu···Cu electrostatic interactions with the incoming CuX.

Table 1. Natural bond order and natural population analyses of **1**–**3** and three units of **4**.

Complex	Wiberg bond index				Natural charge			
	Te–Ru	Ru–Ru	Ru–Cu	Cu–X (X = Cl, Br)	Te	Ru	Cu	X
1	0.33	0.09	0.10	0.32	−0.02	−0.50	+0.58	−0.76
2	0.33	0.09	0.11	0.31	−0.02	−0.50	+0.59	−0.77
3	0.34	0.13	0.09	0.19	+0.14	−0.45[a] −0.33[b]	+0.57	−0.69
4′[c]	0.31	0.09	0.07	0.17 (Br) 0.16 (Cl)	+0.05	−0.53	+0.65	−0.72 (Br) −0.72 (Cl)

[a] In plane. [b] Out of plane. [c] The central unit of three units of **4**.

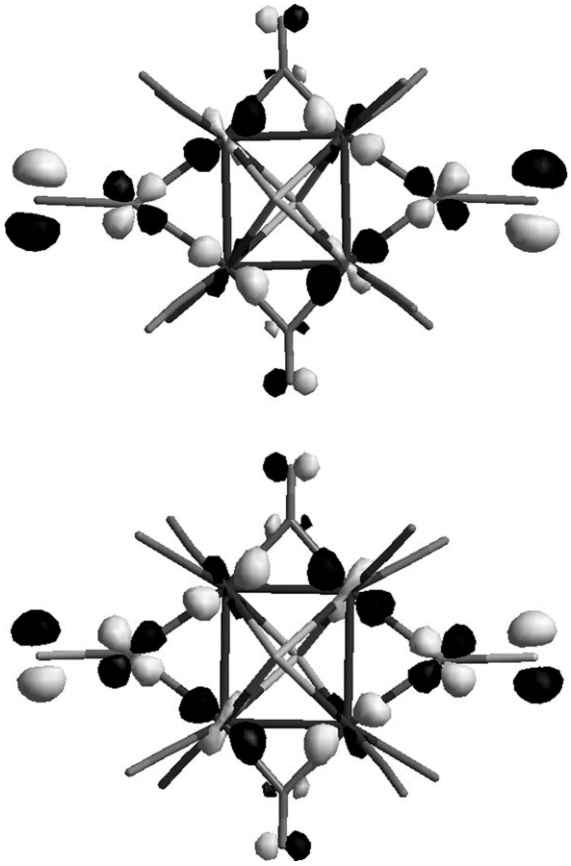

Figure 7. The isosurfaces of the HOMOs of cluster anions **1** (upper) and **2** (lower).

As shown in Figure 7, the HOMO of **1** and **2** has a significant contribution from the p_x and d orbitals of the Ru atoms, the d orbitals of the Cu atoms, and the p_y orbitals of the halides. Thus, it is plausible that the incoming CuX (X = Cl or Br) could interact with the Ru, Cu, and halogen centers of **1** or **2** to form new Cu–Ru and Cu–Cu bonds, accompanied by additional Cu–X and Cu–Te bond formation, to give rise to complex **4**, as evidenced by the fact that **1** or **2** can undergo a coupling reaction with the appropriate CuX to form complex **4**. The coordination number of Cu and X centers is increased in the creation of complex **4** from complexes **1** and **2**. As a result, the Ru–Cu and Cu–X bonds of **4** are weaker than those of **1** or **2**, as well as the Cu–X bond of the incoming CuX, as evidenced by the increase in Ru–Cu and Cu–X distances (Table 2). Complexes **1** and **2** play the role of electron donor in the formation of **4**, while the incoming CuX acts as an electron acceptor. These conclusions are supported by the fact that the HOMO energies of **1** and **2** are higher than the LUMO energies of CuX and the HOMO energy of **4**. Thus, the net charge for the incoming CuX becomes more negative (Table 1) once it is incorporated into complex **4**.

One to six units of compound **4** were calculated to understand why the chain polymer of **4** shows surprising semiconducting properties with a small energy gap of about 0.37 eV. When the chain length increases, the HOMO–LUMO energy gap decreases. In addition, the density of states near the HOMO increases by more than twofold when the number of chain units is increased from one to three. Both effects would be expected to enhance the conductivity when units of complex **4** are polymerized. A close inspection of the HOMOs of complex **4** with one- and three-unit lengths reveals that, except near the Cu and Cl centers, there is almost no change in the HOMO wave function distribution with increasing polymer length (Figure 8). A portion of the probability density near the Cl centers shifts to the Cu centers of adjacent units in the case of a longer chain. In particular, the wave functions for the states near the HOMO

Table 2. Average bond lengths [Å] of $[PPh_4]_2$[**1**], $[PPh_4]_2$[**2**], $[PPh_4]_2$[**3**], $\{[PPh_4]_2$[**4**]·THF$\}_\infty$, and related complexes.

Complex	Te–Ru	Ru–Ru			Ru–Cu	Cu–X [Å] (X = Cl, Br)	Ref.
		CO-bridged	Cu-bridged	Average			
$[PPh_4]_2$[**1**]	2.748	2.7930	3.0257	2.910	2.602	2.267	–[a]
$[PPh_4]_2$[**2**]	2.7487	2.7924	3.0200	2.9062	2.6084	2.144	–[a]
$[PPh_4]_2$[**3**]	2.7077	2.8184	2.9708	2.8755	2.647	2.227	–[a]
$\{[PPh_4]_2$[**4**]·THF$\}_\infty$	2.7479	2.8196	3.0414	2.9305	2.761	2.509 (Br) 2.308 (Cl)	–[a]
$[PPh_4]_2[Te_2Ru_4(CO)_{10}]$	2.723	2.972	–	2.860	–	–	[6d]
$[PPh_4]_2[TeRu_5(CO)_{14}]$	2.698	2.834	–	2.852	–	–	[6d]
$[\{Ru_6Cu_2C(CO)_{16}\}_2Cl_2]^{2-}$	–	2.825	3.030	2.928	2.676	2.190	[9a]

[a] This work.

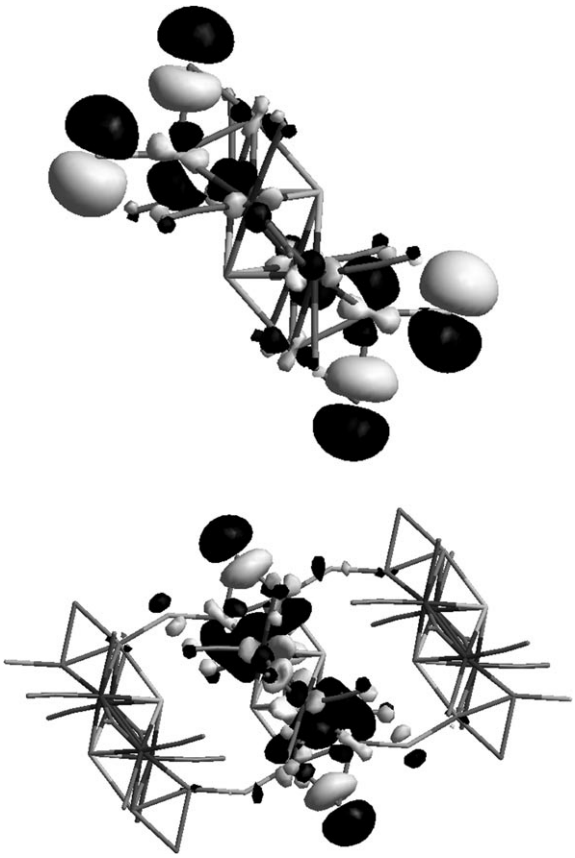

Figure 8. The HOMO for one and three chain units of polymer **4**. Note that only the wave function distribution near the Cu and connecting Cl atoms is affected when the chain is extended from one to three units.

(e.g., HOMO−1 and HOMO−2) are mainly distributed along the -Cu-Cu-Cl- chain among all three units for a longer chain. Therefore, the wave functions of these states are more delocalized. Consequently, the HOMO–LUMO energy gap decreases and the density of states increases with increasing length, as expected from the simple particle-in-a-box model. In addition, the wave function distributions along the -Cu-Cu-Cl- chain should facilitate electron hopping from one unit to nearby units. This is because the wave function overlap for the -Cu-Cu-Cl- chain-distributed states between two adjacent units would be expected to be significant. This hopping effect, along with the small HOMO–LUMO energy gap and the large density of states, explains why the chain polymer **4** shows surprising semiconducting properties with a small energy gap. In summary, the -Cu-Cu-Cl- chain plays an important role in the semiconducting behavior of polymer **4**.

The natural bond order (NBO) and natural population analyses (NPA) for complexes **1**–**3** and the central unit of three units of the polymer of **4** are compared in Table 1. For the Te_2Ru_4-based clusters **1**, **2**, and **4**, each Te atom in polymer **4** carries more positive charge (+0.05) in comparison to the negative charges (−0.02) for each Te atom in **1** and **2**, probably due to the direct interaction of Te with copper halides in the polymer unit. The results show that the Ru atom in **1**, **2**, and **4** carries charges of −0.50, −0.50, and −0.53, and the Cu atom in **1**, **2**, and **4** charges of +0.58, +0.59, and +0.65, suggestive of some degree of ionic interaction between Ru and Cu, which is reflected in their low Wiberg bond indices (0.10, **1**; 0.11, **2**; 0.07, **4**). In addition, relatively small Wiberg bond indices were found for Ru−Ru (0.09, **1**; 0.09, **2**; 0.09, **4**), indicative of the importance of Te−Ru bonds (0.33, **1**; 0.33, **2**; 0.31, **4**) in the stability of the Te_2Ru_4 core of these molecules. On the other hand, the Te atom in $TeRu_5$-based cluster **3** carries more positive charge (+0.14) than those of **1**, **2**, and **4**, mainly owing to the differing metal cores; however, the Cu atom in **3** carries a charge of +0.57, on average, close to those for **1**, **2**, and **4**. In **3**, the coplanar Ru atoms each carry a charge of about −0.45, while the out-of-plane Ru atom carries a charge of −0.33 due to the different bonding situation. Whereas the average Wiberg bond index for Te−Ru (0.34) in **3** is similar to those in **1**, **2**, and **4**, the average Wiberg bond index for Ru−Ru (0.13) in **3** is significantly larger than that for **1**, **2**, and **4** (0.09, 0.09, 0.09), indicative of stronger Ru−Ru bonds in $TeRu_5$-based cluster **3**, which is also consistent with the X-ray data (Table 2).

Structural comparison of $[PPh_4]_2$[1], $[PPh_4]_2$[2], $[PPh_4]_2$[3], and $\{[PPh_4]_2[4]\cdot THF\}_\infty$: The average Te−Ru, Ru−Ru, and Ru−Cu distances in cluster anions **1**–**4** and related compounds are listed in Table 2. The Te−Ru, Ru−Ru, and Ru−Cu distances in **1**–**4** are in good agreement with those of related complexes.[6,9a] The corresponding Te−Ru and Ru−Ru bond lengths of the Te_2Ru_4-based clusters **1**, **2**, and **4** are generally similar. While the Te−Ru distances of **1**, **2**, and **4** are close to that in the related known cluster $[Te_2Ru_4(CO)_{10}]^{2-}$ (2.723 Å),[6d] the Ru−Ru bond lengths are slightly larger than that in $[Te_2Ru_4(CO)_{10}]^{2-}$ (2.860 Å) due to the effect of the bridging copper halides. The average Ru−Ru and Ru−Cu bond lengths of **4** (2.9305 and 2.761 Å) are comparable to those in $[\{Ru_6Cu_2C(CO)_{16}\}_2Cl_2]^{2-}$ (2.928 and 2.676 Å),[9a] but somewhat longer than those in **1** (2.910 and 2.602 Å) and **2** (2.9062 and 2.6084 Å), probably due to the different bonding modes of the copper halides. Further, the Ru−Ru distances in $TeRu_5$-based complex **3** are comparable to those in the related known cluster $[TeRu_5(CO)_{14}]^{2-}$,[6d] but significantly shorter than those in Te_2Ru_4-based clusters **1** and **2**. These phenomena can probably be attributed to better overlap between the Ru atoms in the $TeRu_5$ core, which is consistent with the calculated Wiberg bond indices (Table 1). The average Ru−Ru, Ru−Cu, and Cu−X bond lengths in **4** are longer than those in **1** and **2** due to the higher coordination number of the Ru, Cu, and X centers in **4**.

Conclusion

The first series of Te–Ru–Cu carbonyl complexes was obtained by the use of K_2TeO_3, $[Ru_3(CO)_{12}]$, PPh_4X, and $[Cu(MeCN)_4]BF_4$ or CuX (X = Br, Cl). This system produced

the novel -Cu-Cu-Cl-connected Te–Ru infinite chain polymer, $\{[PPh_4]_2[Te_2Ru_4(CO)_{10}Cu_4Br_2Cl_2]\cdot THF\}_\infty$, which has semiconducting properties with a small band gap of approximately 0.37 eV. Moreover, the rationalized aggregation and semiconducting properties of the chain polymer, as well as the nature of the Te–Ru–Cu clusters, have been discussed on the basis of theoretical calculations. These findings may open new avenues for the construction of Te–Ru–Cu cluster aggregates and infinite frameworks from the viewpoint of both fundamental studies and practical applications.

Experimental Section

All reactions were performed under an atmosphere of pure nitrogen using standard Schlenk techniques.[17] Solvents were purified, dried, and distilled under nitrogen prior to use. K_2TeO_3, $[Ru_3(CO)_{12}]$ (Strem), PPh_4Br, and PPh_4Cl (Acros) were used as received. CuCl and CuBr (Aldrich) were purified by previously published procedures,[18] and $[Cu(MeCN)_4]BF_4$[19] was prepared by previously published methods. Infrared spectra were recorded on a Perkin–Elmer Paragon 500 IR spectrometer as solutions in CaF_2 cells. Elemental analyses for C, H, and N were performed on a Perkin–Elmer 2400 analyzer at the NSC Regional instrumental Center at National Taiwan University, Taipei (Taiwan). Thermogravimetric analyses (TGA) were carried out on a Perkin–Elmer Series-7 system with a heating rate of 5 °C min^{-1} under a nitrogen atmosphere. Powder X-ray diffraction (XRD) data were recorded on a Bruker D8 Avance instrument at 40 kV and 40 mA with $Cu_{K\alpha}$ radiation (λ = 1.54050 Å). ESI-MS spectra were obtained on a Thermo Finnigan LCQ Advantage mass spectrometer.

Synthesis of $[PPh_4]_2[Te_2Ru_4(CO)_{10}Cu_2Br_2]$ ($[PPh_4]_2$[1])

Method 1: MeOH (30 mL) was added to a mixture of $[Ru_3(CO)_{12}]$ (0.729 g, 1.14 mmol) and $K_2TeO_3\cdot H_2O$ (0.310 g, 1.14 mmol). The resulting solution was stirred and heated to reflux for 12 h to give a brown solution, which was filtered. PPh_4Br (0.956 g, 2.28 mmol) was added to the filtrate. The resulting solution was stirred for 1 h, and the solvent removed under vacuum. $[Cu(MeCN)_4]BF_4$ (0.718 g, 2.28 mmol) in MeCN (30 mL) was added to the solid residue over an ice–water bath; the mixture was warmed and stirred at room temperature for another 12 h. The resulting solution was filtered, and the solvent removed under vacuum. The residue was washed with deionized water and Et_2O several times and extracted with CH_2Cl_2 to give a reddish brown solution, and recrystallization from Et_2O/MeOH/CH_2Cl_2 gave $[PPh_4]_2$[**1**]. Yield: 0.89 g, 0.467 mmol, 82 % (based on K_2TeO_3). IR (THF): $\tilde{\nu}_{CO}$ = 1992 (s), 1945 (m), 1798 cm^{-1} (w); ESI-MS (negative ion): m/z calcd for $[M^{2-}+PPh_4^+]^-$: 1567; found: 1565.9; elemental analysis calcd (%) for $[PPh_4]_2$[**1**]: C 36.56, H 2.12, Cu 6.67, Ru 21.2; found: C 36.33, H 2.11, Cu 6.58, Ru 21.1. Brown crystals of $[PPh_4]_2$[**1**] suitable for X-ray analysis were grown from MeCN/MeOH/CH_2Cl_2 at −30 °C. $[PPh_4]_2$[**1**] is soluble in CH_2Cl_2, THF, acetone, and MeCN.

Method 2: MeOH (25 mL) was added to a mixture of $[Ru_3(CO)_{12}]$ (0.360 g, 0.563 mmol) and $K_2TeO_3\cdot H_2O$ (0.153 g, 0.562 mmol). The solution was stirred and heated to reflux for 12 h to give a brown solution which was filtered. PPh_4Cl (0.422 g, 1.13 mmol) was added to the filtrate. The resulting solution was stirred for 1 h, and the solvent removed under vacuum. CuBr (0.485 g, 3.38 mmol) in MeCN (30 mL) was added to the solid over an ice–water bath. The resulting solution was warmed and stirred at room temperature for 12 h, and the solvent was removed under vacuum. The residue was washed with deionized water and Et_2O several times and extracted with CH_2Cl_2, and recrystallization from Et_2O/CH_2Cl_2 gave $[PPh_4]_2$[**1**], as confirmed by IR and ESI-MS measurements. Yield: 0.42 g, 0.22 mmol, 78 % (based on K_2TeO_3).

Method 3: Similar to the procedures described above, the reaction of $K_2TeO_3\cdot H_2O$, $[Ru_3(CO)_{12}]$, PPh_4Br, and CuBr in a molar ratio of 1:1:2:6 gave $[PPh_4]_2$[**1**], which was confirmed by IR spectroscopy, in 70 % yield (based on K_2TeO_3).

Method 4: Similar to the procedures described above, the reaction of $K_2TeO_3\cdot H_2O$, $[Ru_3(CO)_{12}]$, CuBr, and PPh_4Cl in a molar ratio of 1:1:6:2 gave $[PPh_4]_2$[**1**], which was confirmed by IR spectroscopy and ESI-MS, in 58 % yield (based on K_2TeO_3).

Method 5: Similar to the procedures described above, the reaction of $K_2TeO_3\cdot H_2O$, $[Ru_3(CO)_{12}]$, CuBr, and PPh_4Br in a molar ratio of 1:1:6:2 gave $[PPh_4]_2$[**1**], which was confirmed by IR spectroscopy, in 62 % yield (based on K_2TeO_3).

Table 3. Crystallographic data for $[PPh_4]_2$[**1**], $[PPh_4][PPh_4]_2$[**2**], $[PPh_4]_2$[**3**], and $\{[PPh_4]_2$[**4**]$\cdot THF\}_\infty$.

	$[PPh_4]_2$[**1**]	$[PPh_4]^2$[**2**]	$[PPh_4]_2$[**3**]	$\{[PPh_4]_2$[**4**]$\cdot$THF$\}_\infty$
empirical formula	$C_{58}H_{40}Br_2Cu_2O_{10}P_2Ru_4Te_2$	$C_{58}H_{40}Cl_2Cu_2O_{10}P_2Ru_4Te_2$	$C_{76}H_{40}Cl_2Cu_4O_{28}P_2Ru_{10}Te_2$	$C_{62}H_{48}Br_2Cl_2Cu_4O_{11}P_2Ru_4Te_2$
M_r	1905.28	1816.38	3054.07	2175.38
crystal system	triclinic	triclinic	triclinic	monoclinic
space group	$P\bar{1}$	$P\bar{1}$	$P\bar{1}$	$C2/c$
crystal dimensions [mm]	0.14 × 0.08 × 0.02	0.20 × 0.14 × 0.08	0.20 × 0.09 × 0.06	0.26 × 0.10 × 0.06
a [Å]	9.0012(2)	8.9476(2)	9.3570(1)	37.1482(8)
b [Å]	12.9698(3)	12.8267(2)	15.4328(2)	6.8835(1)
c [Å]	14.1598(4)	14.0544(3)	15.9909(3)	26.8490(5)
α [°]	78.4761(9)	77.8361(7)	104.8924(6)	
β [°]	87.0170(9)	87.3720(7)	95.9631(6)	111.9603(8)
γ [°]	71.939(1)	71.495(1)	98.4042(9)	
V [Å^3]	1539.75(7)	1494.88(5)	2183.34(6)	6367.4(2)
Z	1	1	1	4
ρ_{calcd} [g cm^{-3}]	2.055	2.018	2.323	2.269
$\mu(Mo_{K\alpha})$ [mm^{-1}]	3.967	2.838	3.455	4.578
$\lambda(Mo_{K\alpha})$ [Å]	0.71073	0.71073	0.71073	0.71073
T [K]	293(2)	150(2)	240(2)	100(2)
θ range [°]	2.01–24.98	2.02–24.93	2.17–25.01	2.35–25.01
min/max transmission	0.72/0.78	0.59/0.72	0.63/0.70	0.49/0.67
independent reflns [$I > 2\sigma(I)$]	5373 (R_{int} = 0.0750)	5148 (R_{int} = 0.0571)	7661 (R_{int} = 0.0640)	5594 (R_{int} = 0.0565)
parameters	362	361	560	389
$R1$[a]/$wR2$[a] ($I > 2\sigma(I)$)	0.058/0.130	0.032/0.078	0.040/0.090	0.044/0.114
$R1$[a]/$wR2$[a] (all data)	0.107/0.163	0.049/0.093	0.063/0.102	0.052/0.119

[a] The functions minimized during least-squares cycles were $R_1 = \Sigma||F_o| - |F_c||/\Sigma|F_o|$ and $wR_2 = [\Sigma w(F_o^2 - F_c^2)^2/\Sigma w(F_o^2)^2]^{1/2}$.

Synthesis of $[PPh_4]_2[Te_2Ru_4(CO)_{10}Cu_2Cl_2]$ ($[PPh_4]_2$[2]): Similar to method 1 for the preparation of $[PPh_4]_2$[**1**], $[PPh_4]_2$[**2**] was prepared from the reaction of $K_2TeO_3{\cdot}H_2O$, $[Ru_3(CO)_{12}]$, PPh_4Cl, and $[Cu(MeCN)_4][BF_4]$ in a molar ratio of 1:1:2:2. The yield of $[PPh_4]_2$[**2**] was 74% (based on K_2TeO_3). IR (THF): $\tilde{\nu}_{CO}$ = 1992 (s), 1945 (m), 1799 cm^{-1} (w); ESI-MS (negative ion): *m*/*z* calcd for $[M^{2-}+PPh_4^+]^-$: 1478.5; found: 1477.1; elemental analysis calcd (%) for $[PPh_4]_2$[**2**]: C 38.35, H 2.22; found: C 38.54, H 2.42. $[PPh_4]_2$[**2**] is soluble in CH_2Cl_2, THF, and MeCN. Brown crystals of $[PPh_4]_2$[**2**] suitable for X-ray analysis were grown from Et_2O/THF at room temperature.

Synthesis of $[PPh_4]_2[\{TeRu_5(CO)_{14}\}_2Cu_4Cl_2]$ ($[PPh_4]_2$[3])

Method 1: MeOH (25 mL) was added to a mixture of $[Ru_3(CO)_{12}]$ (0.310 g, 0.485 mmol) and $K_2TeO_3{\cdot}H_2O$ (0.128 g, 0.471 mmol). The solution was stirred and heated to reflux for 12 h to give a brown solution, which was filtered. PPh_4Cl (0.357 g, 0.952 mmol) was added to the filtrate. The resulting solution was stirred for 1 h, and the solvent removed under vacuum. CuCl (0.287 g, 2.90 mmol) in MeCN (30 mL) was added to the residue over an ice–water bath. The resulting solution was warmed and stirred at room temperature for 12 h, and the solvent removed under vacuum. The residue was washed with MeOH/deionized water and Et_2O several times and extracted with THF; recrystallization from Et_2O/THF gave $[PPh_4]_2$[**3**]. Yield: 0.19 g, 0.062 mmol, 43% (based on Ru). IR (THF): $\tilde{\nu}_{CO}$ = 2052 (w), 2014 (m), 1996 (s), 1955 (w), 1843 (w), 1828 (w), 1779 cm^{-1} (w); elemental analysis calcd (%) for $[PPh_4]_2$[**3**]: C 29.89, H 1.32; found: C 30.01, H 1.40. $[PPh_4]_2$[**3**] is soluble in CH_2Cl_2, THF, and MeCN. Yellowish brown crystals of $[PPh_4]_2$[**3**] suitable for X-ray analysis were grown from hexane/Et_2O/THF at room temperature.

Method 2: MeOH (25 mL) was added to a mixture of $[Ru_3(CO)_{12}]$ (0.436 g, 0.682 mmol) and $K_2TeO_3{\cdot}H_2O$ (0.184 g, 0.677 mmol). The solution was stirred and heated to reflux for 12 h to give a brown solution, which was filtered, and the solvent removed under vacuum. CuCl (0.415 g, 4.19 mmol) in MeCN (30 mL) was added to the residue in an ice–water bath. The resulting solution was warmed and stirred at room temperature for 12 h, and the solvent removed under vacuum. The solid was treated with PPh_4Br (0.513 g, 1.22 mmol) in MeOH (20 mL) to give a precipitate. The residue was washed with MeOH/deionized water and Et_2O several times and extracted with THF, and recrystallization from Et_2O/THF gave $[PPh_4]_2$[**3**], which was confirmed by IR spectroscopy, ESI-MS, and X-ray analysis. Yield: 0.34 g, 0.11 mmol, 54% (based on Ru).

Method 3: Similar to the procedures described above, the reaction of $K_2TeO_3{\cdot}H_2O$, $[Ru_3(CO)_{12}]$, CuCl, and PPh_4Cl in a molar ratio of 1:1:6:2 gave $[PPh_4]_2[\{TeRu_5(CO)_{14}\}_2Cu_4Cl_2]$ ($[PPh_4]_2$[**3**]), which was confirmed by IR spectroscopy, in a yield of 60% (based on Ru).

Synthesis of $\{[PPh_4]_2[Te_2Ru_4(CO)_{10}Cu_4Br_2Cl_2]{\cdot}THF\}_\infty$ ($\{[PPh_4]_2$[4**]·THF$\}_\infty$)**: MeOH (25 mL) was added to a mixture of $[Ru_3(CO)_{12}]$ (0.303 g, 0.474 mmol) and $K_2TeO_3{\cdot}H_2O$ (0.126 g, 0.464 mmol). The resulting solution was stirred and heated to reflux for 12 h to give a yellowish brown solution, which was filtered. PPh_4Br (0.424 g, 1.01 mmol) was added to the filtrate. The resulting solution was stirred for 1 h, and the solvent removed under vacuum. CuCl (0.295 g, 2.98 mmol) in MeCN (30 mL) was added to the solid over an ice–water bath. The resulting solution was warmed and stirred at room temperature for a further 12 h, and the solvent removed under vacuum. The residue was washed with MeOH/deionized water and Et_2O several times and extracted with MeCN to give a reddish brown solution; recrystallization from MeOH/Et_2O/THF/MeCN at room temperature gave brown crystals that were further washed with THF and MeOH to give $\{[PPh_4]_2$[**4**]·THF$\}_\infty$ (0.25 g, 23% based on $K_2TeO_3{\cdot}H_2O$). IR (Nujol): $\tilde{\nu}_{CO}$ = 1985 (br), 1924 (m), 1793 (w), 1727 cm^{-1} (w); elemental analysis calcd (%) for $\{[PPh_4]_2$[**4**]·THF$\}_\infty$: C 34.23, H 2.22; found: C 34.24, H 2.56. ICP-AES: molar ratio Te:Ru:Cu = 1:2:2. $\{[PPh_4]_2$[**4**]·THF$\}_\infty$ is sparingly soluble in MeCN.

Reaction of $[PPh_4]_2$[1] with CuCl: MeCN (20 mL) was added to a mixture of $[PPh_4]_2$[**1**] (0.350 g, 0.184 mmol) and CuCl (0.038 g, 0.384 mmol) over an ice–water bath. The resulting solution was warmed, stirred at room temperature for 24 h, and worked up as above to give $\{[PPh_4]_2$[**4**]·THF$\}_\infty$ (0.09 g, 23% based on $[PPh_4]_2$[**1**]), which was confirmed by IR spectroscopy and powder XRD pattern, which was in good agreement with that calculated from the single-crystal X-ray diffraction data for $\{[PPh_4]_2$[**4**]·THF$\}_\infty$.

Reaction of $[PPh_4]_2$[2] with CuBr: Similar to the reaction of $[PPh_4]_2$[**1**] with CuCl, $[PPh_4]_2$[**2**] (0.830 g, 0.457 mmol), and CuBr (0.138 g, 0.962 mmol) were used in MeCN (30 mL). A sample of $\{[PPh_4]_2$[**4**]·THF$\}_\infty$ (0.20 g, 21% based on $[PPh_4]_2$[**2**]) was isolated, which was confirmed by IR spectroscopy and powder XRD pattern, which was in good agreement with that calculated from the single X-ray diffraction data of $\{[PPh_4]_2$[**4**]·THF$\}_\infty$.

X-ray structural characterization of $[PPh_4]_2$[1], $[PPh_4]_2$[2], $[PPh_4]_2$[3], and $\{[PPh_4]_2$[4]·THF$\}_\infty$: Crystallographic data for $[PPh_4]_2$[**1**] $[PPh_4]_2$[**2**], $[PPh_4]_2$[**3**], and $\{[PPh_4]_2$[**4**]·THF$\}_\infty$ are given in Table 3, and selected distances and angles are listed in Table 4. All crystals were mounted on glass fibers with epoxy cement. Data for $[PPh_4]_2$[**1**], $[PPh_4]_2$[**2**], $[PPh_4]_2$[**3**], and $\{[PPh_4]_2$[**4**]·THF$\}_\infty$ were collected on a Bruker Nonius Kappa CCD diffractometer using graphite-monochromated $Mo_{K\alpha}$ radiation in the θ–2θ scan mode, and an empirical absorption correction by

Table 4. Selected bond lengths [Å] and angles [°] for $[PPh_4]_2$[**1**], $[PPh_4]_2$[**2**], $[PPh_4]_2$[**3**], and $\{[PPh_4]_2$[**4**]·THF$\}_\infty$.

$[PPh_4]_2$[**1**]			
Te1–Ru1	2.742(1)	Ru1–Ru2a	3.026(1)
Te1–Ru2	2.752(1)	Ru1a–Cu1	2.602(2)
Te1–Ru1a	2.753(1)	Ru2–Cu1	2.602(2)
Te1–Ru2a	2.744(1)	Ru1–Cu1a	2.602(2)
Ru1–Ru2	2.793(1)	Br1–Cu1	2.267(2)
Ru1-Ru2-Ru1a	89.97(3)	Ru2-Cu1-Ru1a	71.11(4)
Ru2-Ru1-Ru2a	90.03(3)	Br1-Cu1-Ru2	140.80(8)
Br1-Cu1-Ru1a	148.05(8)		
$[PPh_4]_2$[**2**]			
Te1–Ru1	2.7511(5)	Ru1–Ru2a	3.0200(5)
Te1–Ru2	2.7460(5)	Ru2–Cu1	2.6084(7)
Te1–Ru2a	2.7537(5)	Ru1a–Cu1	2.6084(7)
Te1–Ru1a	2.7441(5)	Ru1–Cu1a	2.6084(7)
Ru1–Ru2	2.7924(6)	Cu1–Cl1	2.144(2)
Ru1-Ru2-Ru1a	89.92(2)	Ru1a-Cu1-Ru2	70.75(2)
Ru2-Ru1-Ru2a	90.09(2)	Cl1-Cu1-Ru2	141.60(5)
Cl1-Cu1-Ru1a	147.55(5)		
$[PPh_4]_2$[**3**]			
Te1–Ru1	2.6916(6)	Ru4–Ru5	2.9369(7)
Te1–Ru2	2.7216(7)	Ru1–Cu1	2.636(1)
Te1–Ru3	2.7420(6)	Ru1–Cu2	2.6531(9)
Te1–Ru4	2.6755(6)	Ru4–Cu1	2.622(1)
Ru1–Ru2	2.8136(7)	Ru4–Cu2	2.6439(9)
Ru1–Ru4	3.0691(7)	Ru5–Cu2	2.682(1)
Ru1–Ru5	2.9064(7)	Cu1–Cl1a	2.216(2)
Ru2–Ru3	2.8287(7)	Cu1–Cu2	2.608(1)
Ru2–Ru5	2.8306(7)	Cu1–Cu2a	2.779(1)
Ru3–Ru4	2.8128(7)	Cu2–Cl1	2.238(2)
Ru3–Ru5	2.8057(7)		
Cu1-Cu2-Cu1a	74.29(4)	Cu1a-Cl1-Cu2	77.19(5)
Cu2-Cu1-Cu2a	105.71(4)		
$\{[PPh_4]_2$[**4**]·THF$\}_\infty$			
Te1–Ru1	2.7568(7)	Ru1–Cu2	2.781(1)
Te1–Ru1a	2.7314(6)	Ru2–Cu1	2.754(1)
Te1–Ru2	2.7589(7)	Ru2–Cu2	2.784(1)
Te1–Ru2a	2.7446(7)	Cu1–Cu2	2.493(1)
Te1–Cu2	2.8923(9)	Cu1–Br1	2.562(1)
Ru1–Ru2	3.0414(8)	Cu2–Br1	2.455(1)
Ru1–Ru2a	2.8196(7)	Cu1–Cl1	2.294(2)
Ru1–Cu1	2.724(1)	Cu2–Cl1	2.322(2)
Ru2-Ru1-Ru2a	90.28(2)	Ru1-Ru2-Ru1a	89.72(2)
Ru1-Cu1-Ru2	67.46(2)	Ru1-Cu2-Ru2	66.26(2)
Cu2-Br1-Cu1	59.55(3)		

multiscan was applied.[20] The structures were solved by direct methods and were refined with SHELXL-97.[21] All of the non-hydrogen atoms were refined with anisotropic temperature factors. In $\{[PPh_4]_2[\mathbf{4}]\cdot THF\}_\infty$, the hydrogen atoms of the cation were included in calculated positions by using a riding model with fixed C–H distance of 0.960 Å. CCDC 630649 ($[PPh_4]_2[\mathbf{1}]$), 630650 ($[PPh_4]_2[\mathbf{2}]$), 630651 ($[PPh_4]_2[\mathbf{3}]$), and 630652 ($\{[PPh_4]_2[\mathbf{4}]\cdot THF\}_\infty$) contains the supplementary crystallographic data for this paper. These data can be obtained free of charge from The Cambridge Crystallographic Data Centre via www.ccdc.cam.ac.uk/data_request/cif.

Optical properties of $\{[PPh_4]_2[4]\cdot THF\}_\infty$: Near-normal optical reflectance spectra were recorded at room temperature on single-crystal samples. A Bruker IFS 66v Fourier transform infrared spectrometer was used in the far- and mid-infrared regions (80–6000 cm^{-1}), while the near-infrared to near-ultraviolet regions (4000–55000 cm^{-1}) were scanned with a Perkin–Elmer Lambda-900 spectrometer. The modulated light beam from the spectrometer was focused onto either the sample or an Au(Al) reference mirror, and the reflected beam was directed onto a detector appropriate for the frequency range studied. The different sources and detectors used in these studies provided substantial spectral overlap, and the reflectance mismatch between adjacent spectral ranges was less than 1%.

Computational details: Calculations were performed with density functional theory[22] using the Gaussian 03[23] program package. The geometries of complexes **1**–**4** were taken from the crystal structures. All geometries were calculated at the B3LYP/LanL2DZ level. Natural charges[24] and Wiberg bond indices[25] were evaluated with the Weinhold NBO method.[26] Graphical representations of the molecular orbitals were obtained using CS Chem3D 5.0.

Computational details for complexes **1**–**4**, TGA analysis of **4**, and comparison of XRD patterns for **4** are available as Supporting Information.

Acknowledgements

This work was supported by the National Science Council of Taiwan (NSC Grant No. 93-2113M-003-006 to M.S.). We are also grateful to the National Center for High-Performance Computing, where the Gaussian package and computer time were provided. Our gratitude also goes to the Academic Paper Editing Clinic, NTNU.

[1] a) *Metal Clusters in Chemistry* (Eds.: P. Braunstein, L. A. Oro, P. R. Raithby), VCH, Weinheim, **1999**; b) *The Chemistry of Metal Cluster Complexes* (Eds.: D. F. Shriver, H. D. Kaesz, R. D. Adams), VCH, Weinheim, **1990**.

[2] a) S. Leininger, B. Olenyuk, P. J. Stang, *Chem. Rev.* **2000**, *100*, 853; b) O. M. Yaghi, H. Li, C. Davis, D. Richardson, T. L. Groy, *Acc. Chem. Res.* **1998**, *31*, 474; c) D. Braga, F. Grepioni, G. R. Desiraju, *Chem. Rev.* **1998**, *98*, 1375; d) F. A. Cotton, C. Lin, C. A. Murillo, *Acc. Chem. Res.* **2001**, *34*, 759; e) J. K. Bera, K. R. Dunbar, *Angew. Chem.* **2002**, *114*, 4633; *Angew. Chem. Int. Ed.* **2002**, *41*, 4453, and references therein; f) H. D. Selby, B. K. Roland, Z. Zheng, *Acc. Chem. Res.* **2003**, *36*, 933; g) M. Shieh, Y. Liou, M.-H. Hsu, R.-T. Chen, S.-J. Yeh, S.-M. Peng, G.-H. Lee, *Angew. Chem.* **2002**, *114*, 2490; *Angew. Chem. Int. Ed.* **2002**, *41*, 2384; h) K. Uemura, K. Fukui, H. Nishikawa, S. Arai, K. Matsumoto, H. Oshio, *Angew. Chem.* **2005**, *117*, 5595; *Angew. Chem. Int. Ed.* **2005**, *44*, 5459.

[3] a) L. J. Gregoriades, H. Krauss, J. Wachter, A. V. Virovets, M. Sierka, M. Scheer, *Angew. Chem.* **2006**, *118*, 4295; *Angew. Chem. Int. Ed.* **2006**, *45*, 4189; b) M. Scheer, L. J. Gregoriades, A. V. Virovets, W. Kunz, R. Neueder, I. Krossing, *Angew. Chem.* **2006**, *118*, 5818; *Angew. Chem. Int. Ed.* **2006**, *45*, 5689; c) M. Scheer, L. Gregoriades, J. Bai, M. Sierka, G. Brunklaus, H. Eckert, *Chem. Eur. J.* **2005**, *11*, 2163; d) J. Bai, E. Leiner, M. Scheer, *Angew. Chem.* **2002**, *114*, 820; *Angew. Chem. Int. Ed.* **2002**, *41*, 783; e) R. L. Bain, D. F. Shriver, D. E. Ellis, *Inorg. Chim. Acta* **2001**, *325*, 171; f) T. Nakajima, A. Ishiguro, Y. Wakatsuki, *Angew. Chem.* **2001**, *113*, 1096; *Angew. Chem. Int. Ed.* **2001**, *40*, 1066; g) C. Femoni, F. Kaswalder, M. C. Iapalucci, G. Longoni, S. Zacchini, *Chem. Commun.* **2006**, 2135.

[4] a) R. L. Carroll, C. B. Gorman, *Angew. Chem.* **2002**, *114*, 4556; *Angew. Chem. Int. Ed.* **2002**, *41*, 4378; b) D. Wouters, U. S. Schubert, *Angew. Chem.* **2004**, *116*, 2534; *Angew. Chem. Int. Ed.* **2004**, *43*, 2480.

[5] C. Femoni, M. C. Iapalucci, F. Kaswalder, G. Longoni, S. Zacchini, *Coord. Chem. Rev.* **2006**, *250*, 1580.

[6] a) S.-P. Huang, M. G. Kanatzidis, *J. Am. Chem. Soc.* **1992**, *114*, 5477; b) B. K. Das, M. G. Kanatzidis, *Inorg. Chem.* **1995**, *34*, 1011; c) P. Mathur, B. H. S. Thimmappa, A. L. Rheingold, *Inorg. Chem.* **1990**, *29*, 4658; d) B. K. Das, M. G. Kanatzidis, *Polyhedron* **1997**, *16*, 3061; e) A. J. Arce, A. Karam, Y. D. Sanctis, R. Machado, M. V. Capparelli, J. Manzur, *Inorg. Chim. Acta* **1997**, *254*, 119; f) M. Brandl, H. Brunner, H. Cattey, Y. Mugnier, J. Wachter, M. Zabel, *J. Organomet. Chem.* **2002**, *659*, 22.

[7] a) G. Onodera, H. Matsumoto, Y. Nishibayashi, S. Uemura, *Organometallics* **2005**, *24*, 5799; b) P. C. Liao, J. K. Huang, Y. S. Huang, T. R. Yang, *Solid State Commun.* **1996**, *98*, 279.

[8] a) A. Pfitzner, *Chem. Eur. J.* **2000**, *6*, 1891; b) S. Dehnen, A. Eichhöfer, D. Fenske, *Eur. J. Inorg. Chem.* **2002**, 279, and references therein.

[9] a) M. A. Beswick, J. Lewis, P. R. Raithby, M. C. Ramirez de Arellano, *J. Chem. Soc. Dalton Trans.* **1996**, 4033; b) P. R. Raithby in *Transition Metal Clusters* (Ed.: B. F. G. Johnson), Wiley, Chichester, **1980**; c) M. A. Beswick, J. Lewis, P. R. Raithby, M. C. Ramirez de Arellano, *Angew. Chem.* **1997**, *109*, 303; *Angew. Chem. Int. Ed. Engl.* **1997**, *36*, 291; d) M. A. Beswick, J. Lewis, P. R. Raithby, M. C. Ramirez de Arellano, *Angew. Chem.* **1997**, *109*, 2311; *Angew. Chem. Int. Ed. Engl.* **1997**, *36*, 2227.

[10] a) M. Shieh, Y. Liou, S.-M. Peng, G.-H. Lee, *Inorg. Chem.* **1993**, *32*, 2212; b) M. Shieh, P.-F. Chen, S.-M. Peng, G.-H. Lee, *Inorg. Chem.* **1993**, *32*, 3389; c) M. Shieh, Y.-C. Tsai, *Inorg. Chem.* **1994**, *33*, 2303; d) M. Shieh, M.-H. Shieh, Y.-C. Tsai, C.-H. Ueng, *Inorg. Chem.* **1995**, *34*, 5088; e) M. Shieh, T.-F. Tang, S.-M. Peng, G.-H. Lee, *Inorg. Chem.* **1995**, *34*, 2797; f) M. Shieh, C.-m. Sheu, L.-F. Ho, J.-J. Cherng, L.-F. Jang, C.-H. Ueng, S.-M. Peng, G.-H. Lee, *Inorg. Chem.* **1996**, *35*, 5504; g) J.-J. Cherng, Y.-C. Tsai, C.-H. Ueng, G.-H. Lee, S.-M. Peng, M. Shieh, *Organometallics* **1998**, *17*, 255; h) K.-C. Huang, M.-H. Shieh, R.-J. Jang, S.-M. Peng, G.-H. Lee, M. Shieh, *Organometallics* **1998**, *17*, 5202; i) M. Shieh, H.-S. Chen, H.-H. Chi, C.-H. Ueng, *Inorg. Chem.* **2000**, *39*, 5561; j) M. Shieh, H.-S. Chen, Y.-W. Lai, *Organometallics* **2004**, *23*, 4018; k) Y.-W. Lai, J.-J. Cherng, W.-S. Sheu, G.-A. Lee, M. Shieh, *Organometallics* **2006**, *25*, 184.

[11] a) K.-C. Huang, Y.-C. Tsai, G.-H. Lee, S.-M. Peng, M. Shieh, *Inorg. Chem.* **1997**, *36*, 4421; b) M. Shieh, H.-S. Chen, H.-Y. Yang, C.-H. Ueng, *Angew. Chem.* **1999**, *111*, 1339; *Angew. Chem. Int. Ed.* **1999**, *38*, 1252; c) M. Shieh, H.-S. Chen, H.-Y. Yang, S.-F. Lin, C.-H. Ueng, *Chem. Eur. J.* **2001**, *7*, 3152; d) M. Shieh, M.-H. Hsu, *J. Cluster Sci.* **2004**, *15*, 91.

[12] a) J.-J. Cherng, Y.-W. Lai, Y.-H. Liu, S.-M. Peng, C.-H. Ueng, M. Shieh, *Inorg. Chem.* **2001**, *40*, 1206; b) M. Shieh, L.-F. Ho, L-F. Jang, C.-H. Ueng, S.-M. Peng, Y.-H. Liu, *Chem. Commun.* **2001**, 1014; c) M. Shieh, J.-J. Cherng, Y.-W. Lai, C.-H. Ueng, S.-M. Peng, Y.-H. Liu, *Chem. Eur. J.* **2002**, *8*, 4522; d) M. Shieh, R.-L. Chung, C.-H. Yu, M.-H. Hsu, C.-H. Ho, S.-M. Peng, Y.-H. Liu, *Inorg. Chem.* **2003**, *42*, 5477; e) M. Shieh, L.-F. Ho, Y.-W. Guo, S.-F. Lin, Y.-C. Lin, S.-M. Peng, Y.-H. Liu, *Organometallics* **2003**, *22*, 5020; f) M. Shieh, S.-F. Lin, Y.-W. Guo, M.-H. Hsu, Y.-W. Lai, *Organometallics* **2004**, *23*, 5182; g) M.-H. Hsu, R.-T. Chen, W.-S. Sheu, M. Shieh, *Inorg. Chem.* **2006**, *45*, 6740.

[13] R. E. Bachman, K. H. Whitmire, J. van Hal, *Organometallics* **1995**, *14*, 1792.

[14] A. L. Spek, *Acta Crystallogr. Sect. A* **1990**, *46*, C34.

[15] F. Wooten, *Optical Properties of Solids*, Academic Press, New York, **1972**.

[16] a) H. L. Liu, D. B. Tanner, A. E. Pullen, K. A. Abboud, J. R. Reynolds, *Phys. Rev. B* **1996**, *53*, 10557; b) H. L. Liu, L.-K. Chou, K. A. Abboud, B. H. Ward, G. E. Fanucci, G. E. Granroth, E. Canadell,

M. W. Meisel, D. R. Talham, D. B. Tanner, *Chem. Mater.* **1997**, *9*, 1865.
[17] D. F. Shriver, M. A. Drezdon, *The Manipulation of Air-Sensitive Compounds*, Wiley, New York, **1986**.
[18] a) W. L. F. Armarego, D. D. Perrin, *Purification of Laboratory Chemicals*, Butterworth Heinemann, **1997**; b) R. K. Dieter, L. A. Silks III, J. R. Fishpaugh, M. E. Kastner, *J. Am. Chem. Soc.* **1985**, *107*, 4679.
[19] M. G. Simmons, C. L. Merrill, L. J. Wilson, L. A. Bottomley, K. M. Kadish, *J. Chem. Soc. Dalton Trans.* **1980**, 1827.
[20] R. H. Blessing, *Acta Crystallogr. Sect. A* **1995**, *51*, 33.
[21] G. M. Sheldrick, SHELXL97, University of Göttingen, Germany, **1997**.
[22] Gaussian 03, Revision B.04, M. J. Frisch, G. W. Trucks, H. B. Schlegel, G. E. Scuseria, M. A. Robb, J. R. Cheeseman, Jr., J. A. Montgomery, T. Vreven, K. N. Kudin, J. C. Burant, J. M. Millam, S. S. Iyengar, J. Tomasi, V. Barone, B. Mennucci, M. Cossi, G. Scalmani, N. Rega, G. A. Petersson, H. Nakatsuji, M. Hada, M. Ehara, K. Toyota, R. Fukuda, J. Hasegawa, M. Ishida, T. Nakajima, Y. Honda, O. Kitao, H. Nakai, M. Klene, X. Li, J. E. Knox, H. P. Hratchian, J. B. Cross, V. Bakken, C. Adamo, J. Jaramillo, R. Gomperts, R. E. Stratmann, O. Yazyev, A. J. Austin, R. Cammi, C. Pomelli, J. W. Ochterski, P. Y. Ayala, K. Morokuma, G. A. Voth, P. Salvador, J. J. Dannenberg, V. G. Zakrzewski, S. Dapprich, A. D. Daniels, M. C. Strain, O. Farkas, D. K. Malick, A. D. Rabuck, K. Raghavachari, J. B. Foresman, J. V. Ortiz, Q. Cui, A. G. Baboul, S. Clifford, J. Cioslowski, B. B. Stefanov, G. Liu, A. Piskorz, P. Liashenko, I. Komaromi, R. L. Martin, D. J. Fox, T. Keith, M. A. Al-Laham, C. Y. Peng, A. Nanayakkara, M. Challacombe, P. M. W. Gill, B. Johnson, W. Chen, M. W. Wong, C. Gonzalez, J. A. Pople, Gaussian, Inc., Wallingford, CT, **2004**.
[23] a) A. D. Becke, *J. Chem. Phys.* **1993**, *98*, 5648; b) C. Lee, W. Yang, R. G. Parr, *Phys. Rev. B* **1988**, *37*, 785.
[24] a) A. E. Reed, F. Weinhold, *J. Chem. Phys.* **1983**, *78*, 4066; b) A. E. Reed, R. B. Weinstock, F. Weinhold, *J. Chem. Phys.* **1985**, *83*, 735.
[25] K. B. Wiberg, *Tetrahedron* **1968**, *24*, 1083; the Wiberg bond indices (bond orders) are a measure of bond strength.
[26] A. E. Reed, L. A. Curtiss, F. Weinhold, *Chem. Rev.* **1988**, *88*, 899.

Received: January 26, 2007
Published online: May 16, 2007

